Pergamon

0045-7949(95)00019-4

Computers & Structures Vol. 56, No. 2/3, pp. 249–267, 1995

0045-7949/95 $9.50 + 0.00

SOME COMPUTATIONAL ISSUES IN LARGE STRAIN ELASTO-PLASTIC ANALYSIS

G. Gabriel and **K. J. Bathe**

Massachusetts Institute of Technology, Cambridge, MA 02139, U.S.A.

Abstract—The stress integration procedure proposed by Eterovic and Bathe [*Int. J. numer. Meth. Engng* **30**, 1099–1114 (1990).] is studied in detail. The elasto-plasticity formulation is based on the use of the total logarithmic strains and Cauchy stresses, and the Euler backward method of time integration. The accuracy of the procedure is assessed in the solution of various analysis problems and is compared with the accuracy of other schemes. Two important conclusions are reached. First, for a selected level of accuracy, the use of the total strain formulation, in general, allows larger time steps than the use of a stress-rate based formulation (such as a formulation based on the Jaumann stress rate). Second, the original procedure of Eterovic and Bathe can be improved in accuracy by using the trapezoidal rule with a measure to limit the magnitude of the elasto-plastic strain increment per step. This improvement allows for the change of principal stress directions during the incremental step. This capability seems to be unique to this formulation and time integration.

1. INTRODUCTION

Large displacement and large strain inelastic response calculations are pursued to an increasing extent. Most commonly finite element procedures are used. An important basic ingredient in such a solution is the evaluation of the stresses, i.e. when the total strains have been calculated, it is necessary to evaluate the corresponding stresses and material internal variables [2].

In the infinitesimal theory an additive decomposition of the strain rate tensor is used, see Refs [3] and [4].

$$\dot{\epsilon}_{ij} = \dot{\epsilon}^{E}_{ij} + \dot{\epsilon}^{P}_{ij}. \tag{1}$$

Green and Naghdi [5] extended this approach to the finite deformation theory analysis. This formulation was studied by Bathe *et al.* [6], [7] and it was shown that:

- the use of the logarithmic Hencky strain is necessary to ensure isochoric plastic flow;
- the shear modulus is a function of the plastic strain state for certain loading conditions.

Lee [8] introduced a new formulation, based on a conceptual stress relaxed intermediate configuration. If the complete motion of the body of interest is described by the deformation gradient $\mathbf{X}$, then the motion from the initial to the 'stress free' configuration is given by the plastic part of the deformation gradient $\mathbf{X}^{P}$ and the motion from this configuration to the final state is given by $\mathbf{X}^{E}$. Therefore we have

$$\mathbf{X} = \mathbf{X}^{E}\mathbf{X}^{P}. \tag{2}$$

Lee [8] enumerated the difference between the formulations (1) and (2) to be:

- The elastic and plastic parts of the displacements, respectively, are additive. Since the strains are nonlinear expressions in the displacements, they are in general not additive.
- The elastic part of the deformation gradient premultiplies $\mathbf{X}^{P}$ and is only a function of the stress state, while the plastic part is also given by the history of plastic flow. The product (2) is not commutative in general, as are the strains in the additive decomposition.

Of course, for small elastic strains assumptions (1) and (2) are identical.

The stresses are usually obtained by an integral based upon the constitutive equations. In this integration process we can identify two specific difficulties. Firstly, the material rigid rotations need to be integrated accurately, and, secondly, the integration should allow for the change in the principal axes of the stress tensor during each time step.

There are two different approaches. The "rate-type" formulation makes use of the hypoelastic material law, which expresses the time rate of change of the stresses with the time derivative of the strains and rotations. The integration procedure necessary to obtain the total stresses needs to satisfy the criterion of "incremental objectivity", introduced by Hughes and Winget [9] and further elaborated upon by Rashid [10]. This author also introduced the notions of "weak objectivity" which means that the algorithm is objective for special input motions, such as pure rotations or pure stretches, and "strong objectivity"

which means that the algorithm is objective in the presence of both stretches and rotations.

Several procedures have been proposed during recent years to integrate the stresses accurately in rate-type formulations, see also Pinsky *et al.* [11]; Flanagan and Taylor [12]; Weber *et al.* [13]; Nemat-Nasser and Li [14], [15]; and Wang and Atluri [16].

It was demonstrated by Kojić and Bathe [17] that the rate-type approach introduces unphysical residual stresses even for the closed elastic strain paths of a simple plane stress combined tension-shear problem.

A completely different approach is based on using a "total formulation". In this case the criterion of "strong objectivity" is trivially satisfied, because the total stresses are obtained using the total strains, see for an early contribution using this approach Bathe *et al.* [18]. This approach is more reasonable from a physical point of view than the rate-type approach. The question of choosing an incremental stress measure does not require special attention and the formulation of an incrementally objective stress update algorithm is no longer necessary.

For large strain elasto-plastic analysis using "a total formulation" Eterovic and Bathe [1] proposed an efficient algorithm using logarithmic strains to obtain the stress state for a given deformation gradient. The basic idea of this algorithm is to use a hyperelastic approach to determine the elastic predictor stresses exactly,† and then a plastic relaxation process to obtain the final stress state. The applicability of this procedure depends on whether a kinematical decomposition of the deformation gradient into an elastic and plastic part is possible. Furthermore, the plastic evolution equation has to be integrated so that the stress state is obtained from the elastic deformation state at the end of every time step.

There have been several contributions regarding "total formulations" and stress evaluations, see Simo and Ortiz [19]; Simo [20], [21], [22]; Moran *et al.* [23]; Weber and Anand [24]; and Peric [25], [26].

A finite element formulation for finite strain elasto-plastic calculations was given by Dvorkin *et al.* [27].

However, if the principal axes of the stress tensor are changing during the time step all the above procedures produce step-size dependent errors in the direction of the principal axes.

The objective of this work was to study in detail the procedure of Eterovic and Bathe [1], and the procedures of other researchers, compare these techniques and identify possible improvements. Of particular interest is the error introduced due to a change in the principal stress directions.

† In the absence of plastic flow the solution is given at this point without any incremental integration.

2. BASIC EQUATIONS

2.1. *Kinematics*

To describe the elasto-plastic deformation of a body we assume the *deformation gradient* to be multiplicatively decomposable into elastic and plastic parts

$$\mathbf{X} = \mathbf{X}^{\mathrm{E}}\mathbf{X}^{\mathrm{P}} \tag{3}$$

where the superscripts E and P denote the elastic and plastic parts of deformation, respectively. This assumption is widely used in crystal plasticity. Furthermore the *spatial velocity gradient* $\mathbf{L}$ can be written as

$$\mathbf{L} = \dot{\mathbf{X}}\mathbf{X}^{-1} = \mathbf{L}^{\mathrm{E}} + \mathbf{L}^{\mathrm{P}} \tag{4}$$

with

$$\mathbf{L}^{\mathrm{E}} = \dot{\mathbf{X}}^{\mathrm{E}}(\mathbf{X}^{\mathrm{E}})^{-1}$$

$$\mathbf{L}_{\mathrm{P}} = \mathbf{X}^{\mathrm{E}}\dot{\mathbf{X}}^{\mathrm{P}}(\mathbf{X}^{\mathrm{P}})^{-1}(\mathbf{X}^{\mathrm{E}})^{-1}. \tag{5}$$

The velocity gradient can be divided into its symmetric and antisymmetric parts to obtain the *velocity strain tensor* $\mathbf{D}$ and the *spin rate* $\mathbf{W}$

$$\mathbf{L} = \operatorname{sym}\mathbf{L} + \operatorname{skw}\mathbf{L} = \mathbf{D} + \mathbf{W} \tag{6}$$

with

$$\operatorname{sym}\mathbf{L} = \tfrac{1}{2}(\mathbf{L} + \mathbf{L}^{\mathrm{T}})$$

$$\operatorname{skw}\mathbf{L} = \tfrac{1}{2}(\mathbf{L} - \mathbf{L}^{\mathrm{T}}). \tag{7}$$

Since $\det(\mathbf{X}^{\mathrm{P}}) = 1$ and therefore $\det(\mathbf{X}^{\mathrm{E}}) > 0$ the elastic part of the deformation gradient admits the polar decomposition

$$\mathbf{X}^{\mathrm{E}} = \mathbf{R}^{\mathrm{E}}\mathbf{U}^{\mathrm{E}} \tag{8}$$

where $\mathbf{R}^{\mathrm{E}}$ is the orthogonal *elastic rotation tensor* and $\mathbf{U}^{\mathrm{E}}$ is the positive definite, symmetric, *elastic right stretch tensor.*

The elastic strains are defined as

$$\mathbf{E}^{\mathrm{E}} = \ln \mathbf{U}^{\mathrm{E}}. \tag{9}$$

2.2. *Stresses*

The elastic domain is described by the yield condition. For this purpose the *shifted stress deviator* $\mathbf{S}$ is introduced as

$$\mathbf{S} = \mathbf{T}' - \mathbf{B}$$

$$\mathbf{T}' = \operatorname{dev}\mathbf{T}. \tag{10}$$

$\mathbf{T}$ is the *Cauchy stress tensor* and $\mathbf{B}$ is the *back stress tensor* describing the anisotropic resistance to plastic

flow [28] or the kinematic hardening, respectively. The *effective stress* is obtained from the second invariant of $\mathbf{S}$

$$s = \sqrt{\tfrac{3}{2}\mathbf{S}\cdot\mathbf{S}} \tag{11}$$

and the yield surface can be described by the condition

$$\Phi(s,\sigma) = s - \sigma = 0 \tag{12}$$

where σ is called the *deformation resistance* or *yield stress* and $\Phi < 0$ describes the elastic domain. The normal onto the yield surface is given as

$$\mathbf{N} = \sqrt{\frac{3}{2}}\frac{\mathbf{S}}{s}. \tag{13}$$

2.3. *"Rotated quantities"*

For isotropic materials an elastic work conjugate *"rotated" stress tensor* $\bar{\mathbf{T}}$ can be introduced (see e.g. Atluri [29], Hoger [30])

$$\bar{\mathbf{T}}\cdot\dot{\mathbf{E}}^{\mathrm{E}} = J\mathbf{T}\cdot\mathbf{D}^{\mathrm{E}} \tag{14}$$

with the *elastic velocity strain tensor* $\mathbf{D}^{\mathrm{E}} = \operatorname{sym}\mathbf{L}^{\mathrm{E}}$, the Jacobian of the deformation mapping $J = \det\mathbf{X}$ and the Cauchy stress tensor $\mathbf{T}$. We use that the rotated stress tensor and the Hencky strain measure commute

$$[\bar{\mathbf{T}}, \mathbf{E}^{\mathrm{E}}] = \bar{\mathbf{T}}\mathbf{E}^{\mathrm{E}} - \mathbf{E}^{\mathrm{E}}\bar{\mathbf{T}} = 0 \tag{15}$$

and the "rotated" stress tensor can be written as

$$\bar{\mathbf{T}} = J\mathbf{R}^{\mathrm{E}\mathrm{T}}\mathbf{T}\mathbf{R}^{\mathrm{E}}. \tag{16}$$

Similarly the *"rotated" back stress tensor* and the *"rotated" stress deviator* are introduced

$$\bar{\mathbf{B}} = J(\mathbf{R}^{\mathrm{E}})^{\mathrm{T}}\mathbf{B}\mathbf{R}^{\mathrm{E}}$$

$$\bar{\mathbf{S}} = J(\mathbf{R}^{\mathrm{E}})^{\mathrm{T}}\mathbf{S}\mathbf{R}^{\mathrm{E}}. \tag{17}$$

Of course, we also have

$$\bar{\mathbf{S}} = \bar{\mathbf{T}}' - \bar{\mathbf{B}}$$

$$\bar{\mathbf{T}}' = \operatorname{dev}\bar{\mathbf{T}}. \tag{18}$$

The effective stress is then equal to

$$s = J^{-1}\sqrt{\tfrac{3}{2}\bar{\mathbf{S}}\cdot\bar{\mathbf{S}}} \tag{19}$$

and the unit normal onto the yield surface $\bar{\mathbf{N}} = (\mathbf{R}^{\mathrm{E}})^{\mathrm{T}}\mathbf{N}\mathbf{R}^{\mathrm{E}}$ becomes

$$\bar{\mathbf{N}} = \sqrt{\frac{3}{2}}\frac{\bar{\mathbf{S}}}{Js}. \tag{20}$$

The *"modified" plastic velocity gradient* and the *"modified" plastic strain velocity tensor* are given by

$$\bar{\mathbf{L}}_{\mathrm{P}} = (\mathbf{X}^{\mathrm{E}})^{-1}\mathbf{L}^{\mathrm{P}}\mathbf{X}^{\mathrm{E}} = \dot{\mathbf{X}}^{\mathrm{P}}(\mathbf{X}^{\mathrm{P}})^{-1}$$

$$\bar{\mathbf{D}}_{\mathrm{P}} = \operatorname{sym}\bar{\mathbf{L}}^{\mathrm{P}}. \tag{21}$$

The elastic–plastic deformation state is completely described by the following state variables

$$\{\mathbf{X}, \mathbf{X}^{\mathrm{P}}, \mathbf{T}, \sigma, \mathbf{B}\}. \tag{22}$$

These quantities can be replaced equivalently by an associated set of "modified" variables defined by the equations above

$$\{\mathbf{X}, \mathbf{X}^{\mathrm{P}}, \bar{\mathbf{T}}, \sigma, \bar{\mathbf{B}}\}. \tag{23}$$

The stress–strain law is now taken to be

$$\bar{\mathbf{T}} = \mathscr{L}[\mathbf{E}^{\mathrm{E}}] \tag{24}$$

with the fourth-order isotropic elastic material tensor

$$\mathscr{L} = 2\mu\mathbf{I} + (\kappa - \tfrac{2}{3}\mu)\mathbf{1}\otimes\mathbf{1} \tag{25}$$

where $\mathbf{I}$ and $\mathbf{1}$ are the fourth- and second-order identity tensors, respectively. The shear modulus μ and the bulk modulus κ are the elastic constants.

2.4. *Plastic domain–evolution equations*

The evolution equation for the plastic part of the deformation gradient is given by

$$\dot{\mathbf{X}}^{\mathrm{P}} = \bar{\mathbf{L}}^{\mathrm{P}}\mathbf{X}^{\mathrm{P}}. \tag{26}$$

Assuming that the skew-symmetric part of $\bar{\mathbf{L}}^{\mathrm{P}}$ vanishes, or in other words, the elastic spin equals the continuum spin, which is the usual assumption in the theory of isotropic polycrystal metals prior to the development of texture [24, 31 and 32] it follows

$$\dot{\mathbf{X}}^{\mathrm{P}} = \bar{\mathbf{D}}^{\mathrm{P}}\mathbf{X}^{\mathrm{P}}. \tag{27}$$

In the case of the associated flow rule (the classical theory) the direction of plastic flow is taken to be the same as the direction of the outward unit normal onto the yield surface

$$\bar{\mathbf{D}}_{\mathrm{P}} = \operatorname{sym}\bar{\mathbf{L}}^{\mathrm{P}} = \sqrt{\tfrac{3}{2}}\dot{e}^{\mathrm{P}}\bar{\mathbf{N}}. \tag{28}$$

These equations follow directly from the reduced dissipation inequality, for details see e.g. Eterovic and Bathe [33]. It remains to define the evolution equations for the hardening parameters. To describe hardening, use is made of the hardening rules

$$\dot{\sigma} = \beta H\dot{e}^{\mathrm{P}}$$

$$\overset{\bullet}{\bar{\mathbf{B}}} = \tfrac{2}{3}(1-\beta)H\bar{\mathbf{D}}^{\mathrm{P}} \tag{29}$$

with the *hardening modulus* H and the *hardening ratio* β considered as functions of the *equivalent plastic strain* e^P

$$H = H(e^P)$$

$$\beta = \beta(e^P). \tag{30}$$

We have isotropic hardening when $\beta = 1$ and kinematic hardening when $\beta = 0$. The more general description in eqn (29) corresponds to mixed hardening.

3. COMPUTATIONAL PROCEDURE

The complete computational procedure consists of:

(1) The stable, accurate and efficient integration of the plastic evolution eqn (27) to obtain the final stress state at the end of the time step.

(2) The calculation of a consistent tangent matrix used in the Newton (or some other) iteration process.

We note that the first item is essential for solving the given problem accurately, while the second item improves the convergence of the iteration process and may also decide whether an actual engineering problem can or cannot be solved.

In this paper we consider the integration of the stresses. It is assumed that the variables are given for the converged configuration at time t

$$\{{}_0^t\mathbf{X}, {}_0^t\mathbf{X}^P, {}^t\bar{\mathbf{T}}, {}^t\sigma, {}^t\bar{\mathbf{B}}\}. \tag{31}$$

The objective of the time integration algorithm is to calculate corresponding to the given deformation gradient ${}_0^{t+\Delta t}\mathbf{X}$ the remaining variables for the updated configuration at time $t + \Delta t$

$$\{{}_0^{t+\Delta t}\mathbf{X}, {}_0^{t+\Delta t}\mathbf{X}^P, {}^{t+\Delta t}\bar{\mathbf{T}}, {}^{t+\Delta t}\sigma, {}^{t+\Delta t}\bar{\mathbf{B}}\}. \tag{32}$$

The proposed integration procedure corresponds to the algorithm of Eterovic and Bathe [1], but a simple refinement allows for the rotation of the principal axes of the stress tensor during the time increment. The result is that larger time steps can be used in some analyses.

3.1. *Kinematics*

Consider the evolution equation of the plastic deformation gradient, equation (27)

$$\dot{\mathbf{X}}^P(t) = \bar{\mathbf{D}}^P(t)\mathbf{X}^P(t). \tag{33}$$

† Note that in this case ${}^t\mathbf{U}^E$ and $\bar{\mathbf{D}}^P$ have the same eigendirections during the time step $t \leqslant \tau \leqslant t + \Delta t$, both are symmetric and their product is still symmetric.

The general solution of this differential equation is

$${}_0^{t+\Delta t}\mathbf{X}^P = \left(\exp\left(\int_t^{t+\Delta t} \bar{\mathbf{D}}^P(\tau)\,d\tau\right)\right){}_0^t\mathbf{X}^P. \tag{34}$$

Taking the inverse and premultiplying with ${}_0^{t+\Delta t}\mathbf{X}$ we obtain

$${}_0^{t+\Delta t}\mathbf{X}^E = \mathbf{X}_*^E \exp\left(-\int_t^{t+\Delta t} \bar{\mathbf{D}}^P(\tau)\,d\tau\right) \tag{35}$$

where $\mathbf{X}_*^E$ is the *trial elastic deformation gradient*

$$\mathbf{X}_*^E = {}_0^{t+\Delta t}\mathbf{X}\,({}_0^t\mathbf{X}^P)^{-1}. \tag{36}$$

Also, the final elastic deformation state can be written as

$${}_0^{t+\Delta t}\mathbf{X}^E = {}_0^{t+\Delta t}\mathbf{X}({}_0^{t+\Delta t}\mathbf{X}^P)^{-1}. \tag{37}$$

Since $\det(\mathbf{X}_*^E) > 0$ and $\det({}_0^{t+\Delta t}\mathbf{X}^E) > 0$ we have the polar decompositions

$${}_0^{t+\Delta t}\mathbf{X}^E = {}_0^{t+\Delta t}\mathbf{R}^E\,{}_0^{t+\Delta t}\mathbf{U}^E$$

$$\mathbf{X}_*^E = \mathbf{R}_*^E\mathbf{U}_*^E. \tag{38}$$

It follows from eqn (35) using eqns (36) to (38) that

$$\mathbf{R}_*^E\mathbf{U}_*^E = {}_0^{t+\Delta t}\mathbf{R}^E\,{}_0^{t+\Delta t}\mathbf{U}^E \exp\left(\int_t^{t+\Delta t} \bar{\mathbf{D}}^P(\tau)\,d\tau\right). \tag{39}$$

From eqns (18), (20) and (28) we have

$$[\bar{\mathbf{D}}^P, \bar{\mathbf{S}}] = [\bar{\mathbf{D}}^P, (\bar{\mathbf{T}}' - \bar{\mathbf{B}})]$$

$$= [\bar{\mathbf{D}}^P, \bar{\mathbf{T}}'] + [\bar{\mathbf{B}}, \bar{\mathbf{D}}^P] = 0. \tag{40}$$

For a motion with constant principal stress directions it follows from (29b)

$$[\bar{\mathbf{B}}, \bar{\mathbf{D}}^P] = 0. \tag{41}$$

For isotropic materials the material stress deviator commutes with the elastic part of the strains (15) and it follows

$$[\bar{\mathbf{T}}', \mathbf{E}^E] = 0. \tag{42}$$

Because of $[\mathbf{E}^E, \mathbf{U}^E] = 0$ we finally have

$$[\bar{\mathbf{D}}^P, \mathbf{U}^E] = 0. \tag{43}$$

This equation holds for all times during the deformation process. Thus, it follows that the trial elastic rotation tensor is equal to the final elastic rotation tensor for every motion with constant principal axes of the stress tensor†

$$\mathbf{R}_*^E = {}_0^{t+\Delta t}\mathbf{R}^E \tag{44}$$

and therefore

$$\mathbf{U}_*^{\mathrm{E}} = {}^{t+\Delta t}_{0}\mathbf{U}^{\mathrm{E}} \exp\left(\int_t^{t+\Delta t} \bar{\mathbf{D}}^{\mathrm{P}}(\tau)\, d\tau\right). \tag{45}$$

If the principal axes of the stress tensor are changing, it follows from eqn (39) using the Hencky strain law that

$${}^{t+\Delta t}_{0}\mathbf{R}^{\mathrm{E}} = \mathbf{R}_*^{\mathrm{E}} \exp(\mathbf{E}_*^{\mathrm{E}}) \exp\left(-\int_t^{t+\Delta t} \bar{\mathbf{D}}^{\mathrm{P}}(\tau)\, d\tau\right) \times \exp(-{}^{t+\Delta t}_{0}\mathbf{E}^{\mathrm{E}}). \tag{46}$$

We can show that for total elastic strains occurring in most practical calculations (up to 10%) the product of the exponential terms on the right-handside is approximately equal to the identity. Hence, with an acceptable error, eqns (44) and (45) can still be used, see Appendix.

3.2. *Stresses*

Using the Hencky strain measure we obtain from eqn (45)

$$\mathbf{E}_*^{\mathrm{E}} = {}^{t+\Delta t}_{0}\mathbf{E}^{\mathrm{E}} + \int_t^{t+\Delta t} \bar{\mathbf{D}}^{\mathrm{P}}(\tau)\, d\tau. \tag{47}$$

Following Eterovic and Bathe [1] and using the elastic stress–strain law (24) we obtain the evolution equation for the "rotated" stress deviator

$${}^{t+\Delta t}\bar{\mathbf{T}}' = \bar{\mathbf{T}}'_* - 2\mu \int_t^{t+\Delta t} \bar{\mathbf{D}}^{\mathrm{P}}(\tau)\, d\tau \tag{48}$$

and using the mean stress

$$\mathrm{tr}\,{}^{t+\Delta t}\bar{\mathbf{T}} = \mathrm{tr}\,\bar{\mathbf{T}}_* = 3\kappa\ \mathrm{tr}\,\mathbf{E}_*^{\mathrm{E}}. \tag{49}$$

The "rotated" stress tensor is equal to

$${}^{t+\Delta t}\bar{\mathbf{T}} = {}^{t+\Delta t}\bar{\mathbf{T}}' + \tfrac{1}{3}(\mathrm{tr}\,{}^{t+\Delta t}\bar{\mathbf{T}})\mathbf{1}. \tag{50}$$

We note again that eqn (48) is an approximation if the principal axes of the stress tensor are changing during the deformation. However, this equation can still be used for a moderate amount of elastic strains and sufficiently small time steps. The proof and some remarks about suggested time steps are given in the Appendix.

3.3. *Integration procedure*

Further attention is now focussed on solving the integral in eqn (48). From eqn (28) we obtain

$$\int_t^{t+\Delta t} \bar{\mathbf{D}}^{\mathrm{P}}(\tau)\, d\tau = \sqrt{\frac{3}{2}} \int_t^{t+\Delta t} \dot{e}^{\mathrm{P}}(\tau)\bar{\mathbf{N}}(\tau)\, d\tau. \tag{51}$$

We assume that the time derivative of the equivalent plastic strain is constant and equal to

$$\dot{e}^{\mathrm{P}}(\tau) = \frac{{}^{t+\Delta t}e^{\mathrm{P}} - {}^{t}e^{\mathrm{P}}}{\Delta t} = \text{const.} \tag{52}$$

Further we assume that

$$\int_t^{t+\Delta t} \mathbf{N}(\tau)\, d\tau \cong \Delta t\ {}^{t+\alpha\Delta t}\bar{\mathbf{N}} \tag{53}$$

where α is the Euler method integration parameter. Then eqn (51) becomes

$$\int_t^{t+\Delta t} \bar{\mathbf{D}}^{\mathrm{P}}(\tau)\, d\tau = \tfrac{3}{2}({}^{t+\Delta t}e^{\mathrm{P}} - {}^{t}e^{\mathrm{P}}) \frac{{}^{t+\alpha\Delta t}\bar{\mathbf{S}}}{{}^{t+\alpha\Delta t}(Js)} \tag{54}$$

and

$${}^{t+\alpha\Delta t}\bar{\mathbf{S}} = (1-\alpha)\,{}^{t}\mathbf{S} + \alpha\ {}^{t+\Delta t}\bar{\mathbf{S}}. \tag{55}$$

Using the hardening rule eqn (29a), eqn (52) and the consistency condition $\dot{s} = \dot{\sigma}$ we have

$${}^{t+\Delta t}s = {}^{t+\Delta t}\sigma = {}^{t}\sigma + ({}^{t+\Delta t}e^{\mathrm{P}} - {}^{t}e^{\mathrm{P}})\,{}^{t+\Delta t}\beta\ {}^{t+\Delta t}H. \tag{56}$$

These equations yield

$$\int_t^{t+\Delta t} \bar{\mathbf{D}}^{\mathrm{P}}(\tau)\, d\tau = q[(1-\alpha)\,{}^{t}\bar{\mathbf{S}} + \alpha\ {}^{t+\Delta t}\bar{\mathbf{S}}] \tag{57}$$

with

$$q = \frac{\tfrac{3}{2}\,{}^{t+\Delta t}e^{\mathrm{P}} - {}^{t}e^{\mathrm{P}}}{{}^{t}J\,{}^{t}s - \alpha\,{}^{t}J\,{}^{t}s + \alpha\,{}^{t+\Delta t}J\,{}^{t}s + \alpha\,{}^{t+\Delta t}J({}^{t+\Delta t}e^{\mathrm{P}} - {}^{t}e^{\mathrm{P}})\,{}^{t+\Delta t}\beta\ {}^{t+\Delta t}H}. \tag{58}$$

Using the hardening rule eqn (29b), we have

$${}^{t+\Delta t}\bar{\mathbf{B}} = {}^{t}\bar{\mathbf{B}} + \frac{2}{3}\int_t^{t+\Delta t} (1-\beta)H\bar{\mathbf{D}}^{\mathrm{P}}(\tau)\, d\tau. \tag{59}$$

Assuming that the hardening parameters are constant during the time step and equal to

$$\beta = {}^{t+\Delta t}\beta$$
$$H = {}^{t+\Delta t}H \tag{60}$$

we have

$${}^{t+\Delta t}\bar{\mathbf{B}} = {}^{t}\bar{\mathbf{B}} + \tfrac{2}{3}(1 - {}^{t+\Delta t}\beta)\,{}^{t+\Delta t}H \int_t^{t+\Delta t} \bar{\mathbf{D}}^{\mathrm{P}}(\tau)\, d\tau. \tag{61}$$

Combining eqns (18), (48) and (61) yields

$$(\bar{\mathbf{T}}'_* - {}^{t}\bar{\mathbf{B}}) = ({}^{t+\Delta t}\bar{\mathbf{T}}' - {}^{t+\Delta t}\bar{\mathbf{B}}) + [2\mu + \tfrac{2}{3}(1 - {}^{t+\Delta t}\beta)\,{}^{t+\Delta t}H] \int_t^{t+\Delta t} \bar{\mathbf{D}}^{\mathrm{P}}(\tau)\, d\tau. \tag{62}$$

The left hand side corresponds to a trial elastic stress deviator $\bar{\mathbf{S}}_*$ and using eqn (57) we obtain for general hardening

$$\bar{\mathbf{S}}_* = {}^{t+\Delta t}\bar{\mathbf{S}} + c[(1-\alpha){}^{t}\bar{\mathbf{S}} + \alpha\, {}^{t+\Delta t}\bar{\mathbf{S}}] \tag{63}$$

where

$$c = \frac{[3\mu + (1 - {}^{t+\Delta t}\beta)\,{}^{t+\Delta t}H]({}^{t+\Delta t}e^{\mathrm{P}} - {}^{t}e^{\mathrm{P}})}{{}^{t}J\,{}^{t}s - \alpha\,{}^{t}J\,{}^{t}s + \alpha\,{}^{t+\Delta t}J\,{}^{t}s + \alpha\,{}^{t+\Delta t}J({}^{t+\Delta t}e^{\mathrm{P}} - {}^{t}e^{\mathrm{P}})\,{}^{t+\Delta t}\beta\,{}^{t+\Delta t}H}. \tag{64}$$

Therefore

$${}^{t+\Delta t}\bar{\mathbf{S}} = \frac{1}{1+\alpha c}\,[\bar{\mathbf{S}}_* - (1-\alpha)c\,{}^{t}\bar{\mathbf{S}}]. \tag{65}$$

The solution of eqn (65) has to be obtained by satisfying the yield condition (12), and this results in the *effective-stress-function equation* [2]

$$\Phi({}^{t+\Delta t}e^{\mathrm{P}}) = \frac{1}{{}^{t+\Delta t}J}\sqrt{\tfrac{3}{2}\,{}^{t+\Delta t}\bar{\mathbf{S}}({}^{t+\Delta t}e^{\mathrm{P}})\cdot{}^{t+\Delta t}\bar{\mathbf{S}}({}^{t+\Delta t}e^{\mathrm{P}})} - {}^{t+\Delta t}\sigma({}^{t+\Delta t}e^{\mathrm{P}}) = 0. \tag{66}$$

This equation can be solved numerically using a simple bisection algorithm, a Newton method or a secant method. The above computational solution is the one given by Eterovic and Bathe when $\alpha = 1$ is used. Using $\alpha = 1$ we assume that the principal stress directions of the second term in equation (48) are the same as the principal directions of the other terms in that equation. Thus the directions of the final state are determined by the trial state. The solution is exact using the radial return method if the principal stress directions do not change during the step. In this solution process rigid body rotations do not affect the accuracy.

If the principal stress directions (with rigid body rotations removed) change during the step an error is introduced during the time integration. This error depends on the step size.

To reduce this integration error the parameter $\alpha = \frac{1}{2}$ can be employed. Namely using $\alpha = \frac{1}{2}$ we allow for the change in the principal axes of the stress tensor during the time increment and can expect a better performance of the algorithm when such changes are significant. Of course, in elastic analysis, no such error occurs, irrespective of how large the change in principal stress directions is during the time step. We demonstrate these theoretical observations in the example solutions presented next.

4. NUMERICAL EXAMPLES

We note that our algorithm yields accurate results according to the analytical solutions given in the Refs [10–12, 26] for pure elastic deformations and any amount of rigid rotation. Thus, there is no need to show such solutions. Furthermore, we note that using our procedure the value of the integration parameter α does not enter the elastic solution process.

In this section we demonstrate the performance of the proposed algorithm in large deformation elastic–plastic analysis. We use a norm η as a measure to evaluate the accuracy of our solution. This norm is taken to be (see Appendix)

$$\eta = \frac{\left\| \int_t^{t+\Delta t} \bar{\mathbf{D}}^{\mathrm{P}}(\tau)\,\mathrm{d}\tau \right\|}{\| {}^{t+\Delta t}_{0}\mathbf{E}^{\mathrm{E}} \|} \tag{67}$$

and determines a ratio between the plastic strain increment and the total elastic strains. In our calculations we used the spectral norm, see Ref. [2]. We also give a value marked $\eta_{\text{max. allowable}}$, which was obtained according to eqn (94).

Of course, the value of the integration parameter α will now affect the accuracy of the numerical results. If not mentioned otherwise the material parameters used in the example solutions are

Shear modulus μ	76.92 MPa
Bulk modulus κ	166.67 MPa
Yield stress σ_0	0.75 MPa
Hardening modulus H	2.00 MPa.

(68)

4.1. *Simple transverse displacements without hardening*

We consider an in-plane isochoric deformation with no hardening according to the deformation gradient

$$\mathbf{X} = \begin{bmatrix} 1 & \dot{\gamma}t & 0 \\ 0 & 1 & 0 \\ 0 & 0 & 1 \end{bmatrix} \tag{69}$$

with $\dot{\gamma}$ a constant, $\gamma = \dot{\gamma}t$ and $0 \leqslant t \leqslant 1$.

The analytical solution for this problem using the Jaumann rate based formulation is given for instance by Weber *et al.* [13] (see also Moss [34]). For convenience the deformation resistance against shear is denoted as $k = \sigma_0/\sqrt{3}$. For sufficiently small values of $\dot{\gamma}t$ the material behavior is elastic and the stress components are

$$T_{12} = \mu \sin(\dot{\gamma}t)$$

$$T_{11} = \mu(1 - \cos(\dot{\gamma}t)) = -T_{22}. \tag{70}$$

Yielding occurs at time t_0

$$t_0 = \frac{1}{\dot{\gamma}} \arccos\left[1 - \frac{1}{2}\left(\frac{k}{\mu}\right)^2\right]. \tag{71}$$

Then for $t > t_0$ the elastic–plastic solution is given by

$$T_{12} = k \cos \Psi$$

$$T_{11} = k \sin \Psi = -T_{22} \tag{72}$$

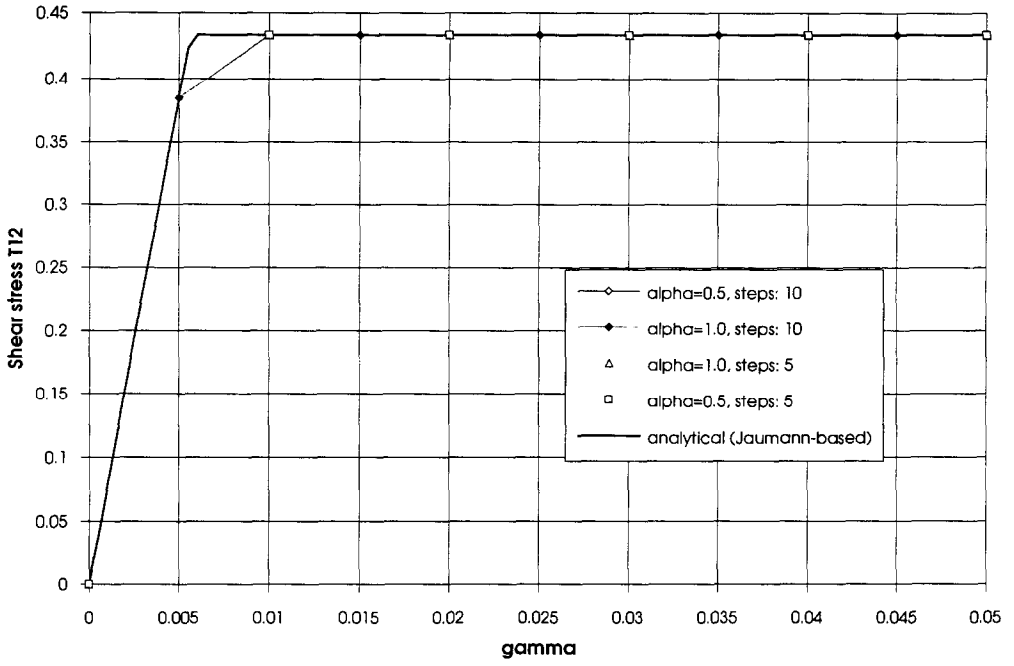

Fig. 1. Simple transverse displacements without hardening, small deformations, shear stresses T12 (all stresses are nearly the same).

with

$$\Psi = \left[\frac{k}{\mu} + \left(\Psi_0 - \frac{k}{\mu}\right)\exp\left(-\frac{\mu}{k}\dot{\gamma}(t - t_0)\right)\right]$$

$$\Psi_0 = \arcsin\left(\frac{1}{2}\frac{k}{\mu}\right). \tag{73}$$

We obtained results using $\alpha = 1$ and $\alpha = \frac{1}{2}$ as integration parameters, and compared our numerical solution with the analytical solution of eqn (72), but of course such comparison is only valid for small deformations.

The shear and normal stresses and the norm η for $\dot{\gamma} = 0.05$ are shown in Figs 1–3. This region

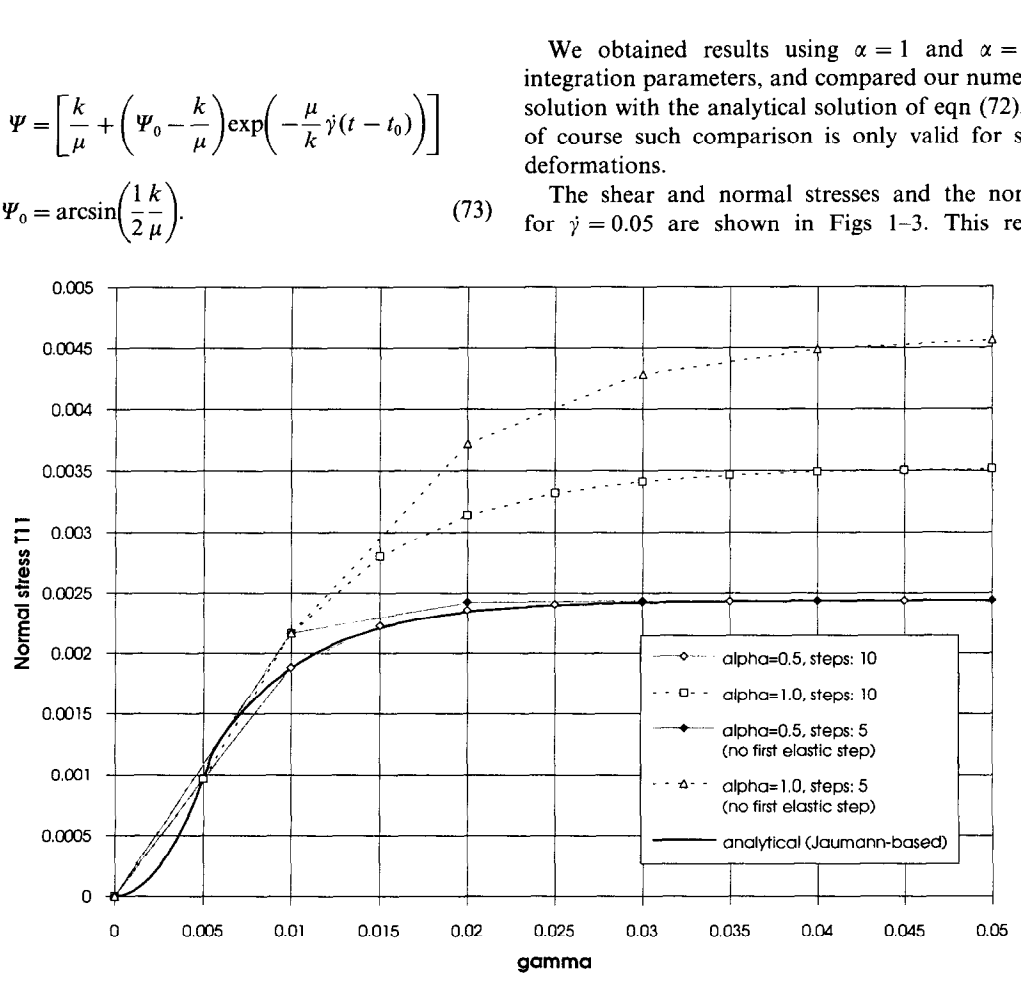

Fig. 2. Simple transverse displacements without hardening, small deformations, normal stresses T11.

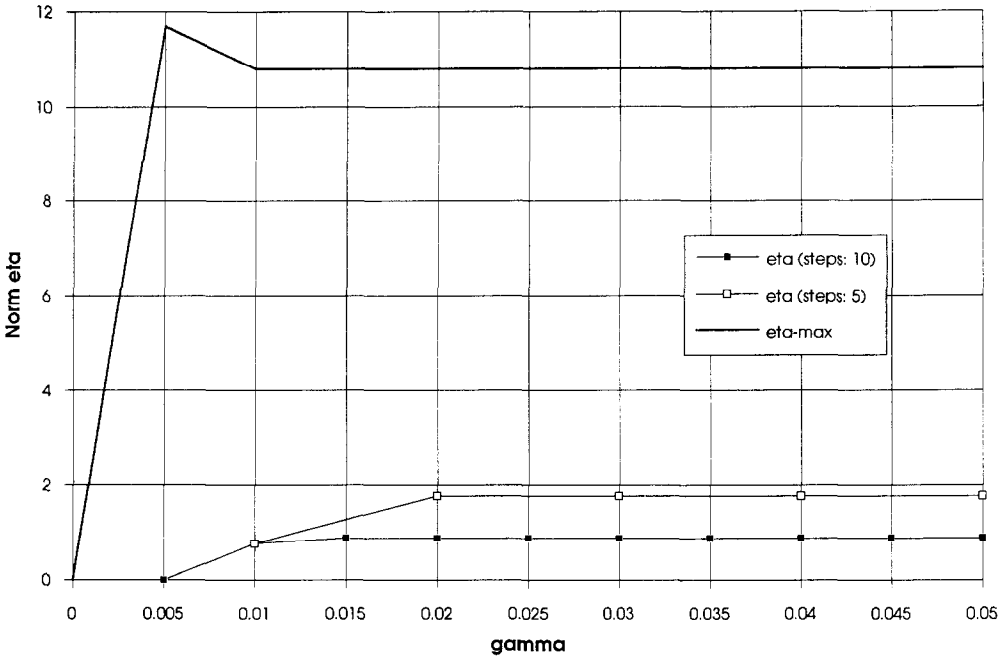

Fig. 3. Simple transverse displacements without hardening, norm η for $\alpha = 1/2$ and 1 (ratio between plastic strain increment and total elastic strain).

corresponds to small deformations, where the elastic and plastic parts of deformation are nearly of the same order.

Larger deformations are dominated by plasticity. Figures 4–6 show the results for $\dot{\gamma} = 0.5$.

We note that at large deformations the normal stresses are one to two orders of magnitude smaller than the shear stresses. The shear stresss are always accurately predicted, even with large solution steps, and using $\alpha = 1$ and $\alpha = \frac{1}{2}$. However, the second-order normal stresses are much better approximated when using $\alpha = \frac{1}{2}$ and Δt within the recommended time step region ($\eta \leqslant 2$). For larger time steps the solution using $\alpha = \frac{1}{2}$ starts to oscillate around the

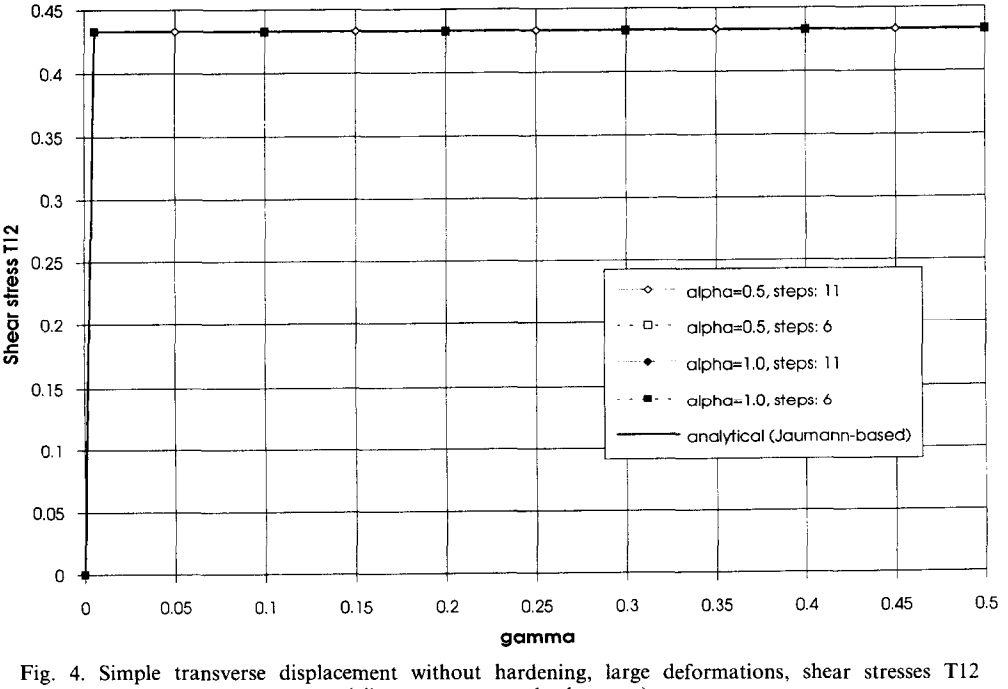

Fig. 4. Simple transverse displacement without hardening, large deformations, shear stresses T12 (all stresses are nearly the same).

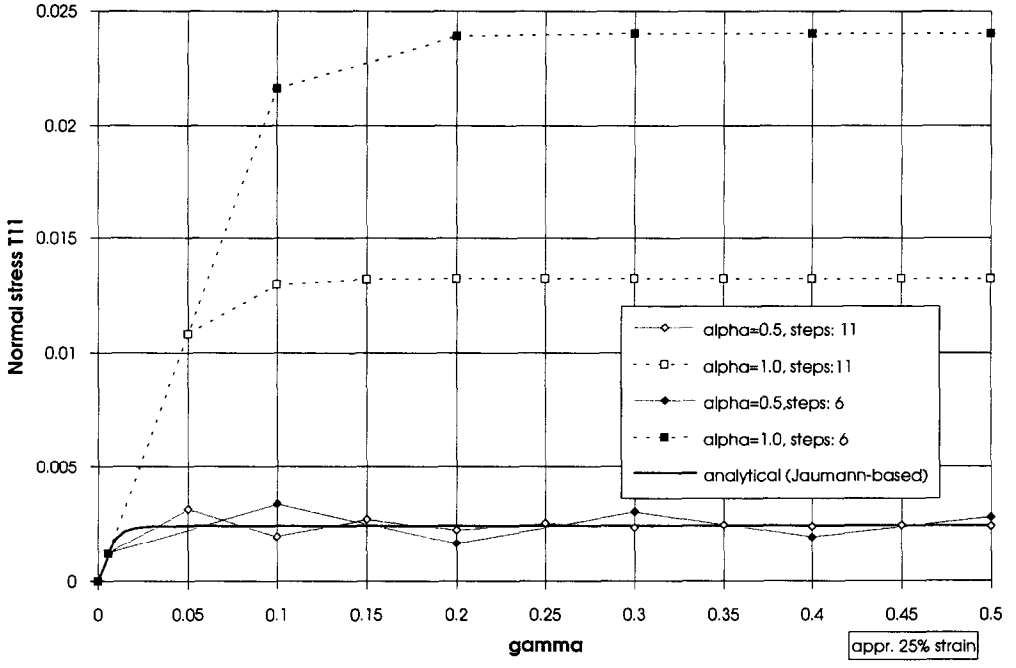

Fig. 5. Simple transverse displacement without hardening, large deformations, normal stress T11.

analytical value and the solution using $\alpha = 1$ drifts away from this solution. Of course, the yield condition is always satisfied.

The reason for this behavior is given by the rotation of the principal axes of the stress tensor during the deformation.

4.2. *Simple transverse displacements with both isotropic and kinematic hardening*

We use again the material parameters given in eqn (68) and use the deformation according to eqn (69) with $\dot{\gamma} = 1$, $\gamma = \dot{\gamma}t$ and $0 \leqslant t \leqslant 1$. This

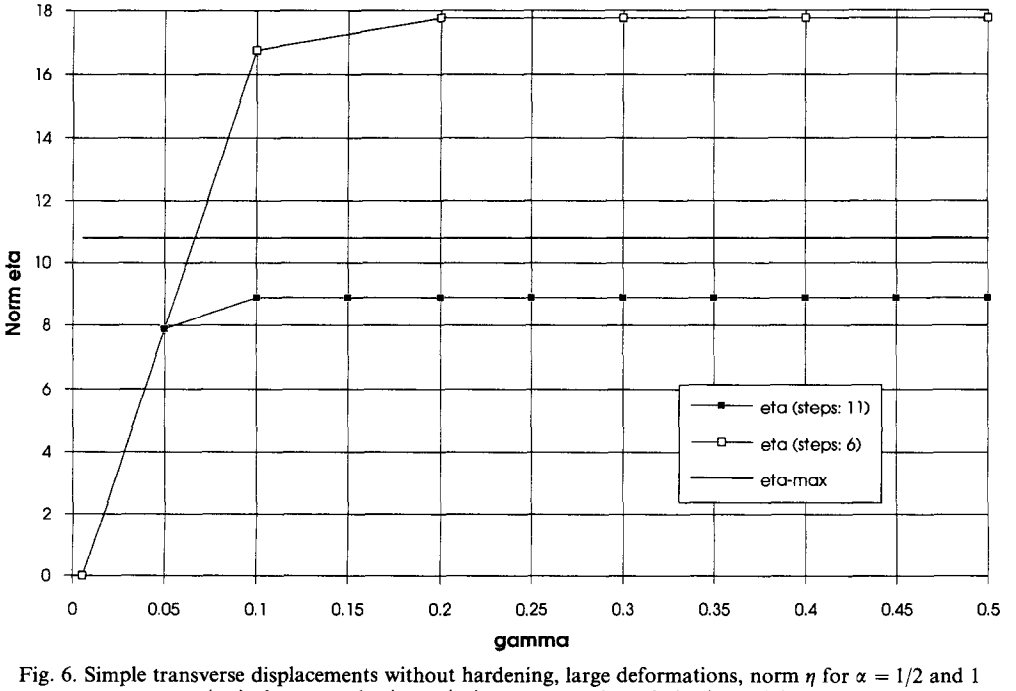

Fig. 6. Simple transverse displacements without hardening, large deformations, norm η for $\alpha = 1/2$ and 1 (ratio between plastic strain increment and total elastic strain).

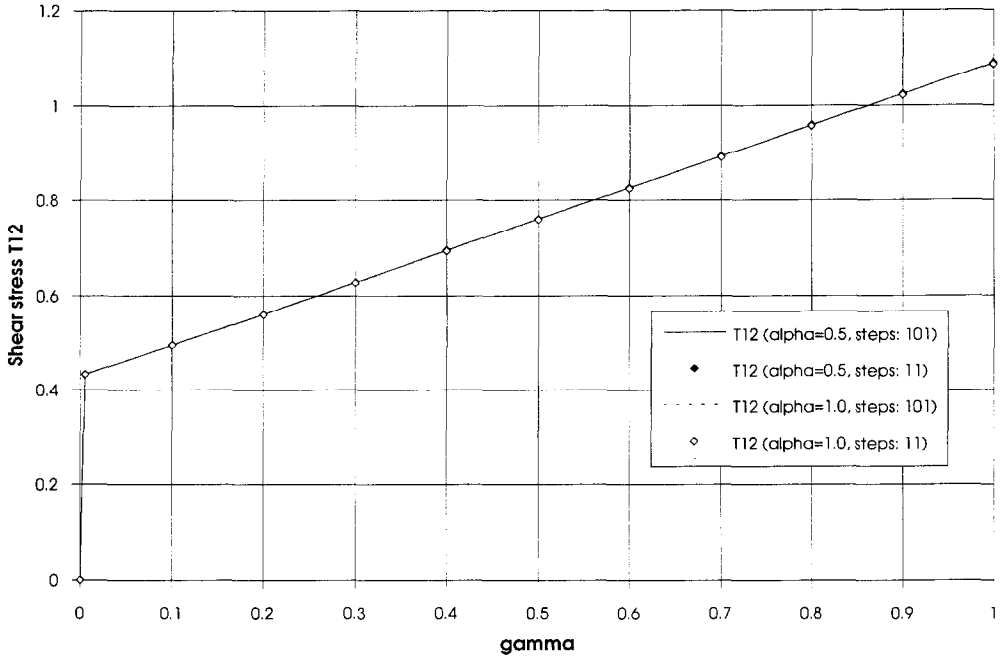

Fig. 7. Simple transverse displacements with isotropic hardening, shear stresses T12 (all stresses are nearly the same).

corresponds to a maximum principal strain of 48%. The results for isotropic and kinematic hardening, using small and large time-steps are given in Figs 7–9 and in Figs 10–12. An analytical solution is not given, but it is obvious that the solutions using $\alpha = \frac{1}{2}$ and $\alpha = 1$ converge to the solution using $\alpha = \frac{1}{2}$ obtained with small time steps. The norm η is again a good measure of the size of the incremental steps in the solution process. The maximum allowable value of η (marked $\eta_{\text{max. allowable}}$) was obtained according to eqn (94).

To illustrate the performance of our solution algorithm for very large deformations we include the results for a simple transverse displacement process of a pure iron specimen. Referring to Refs [35] and [36] we conclude that the maximum possible

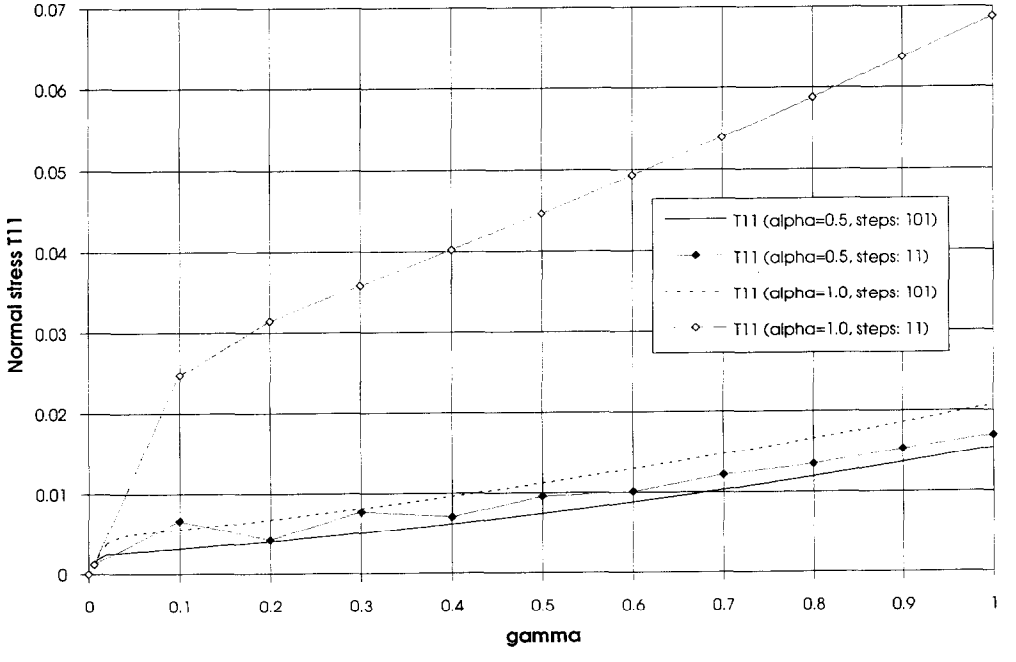

Fig. 8. Simple transverse displacements with isotropic hardening, normal stresses T11.

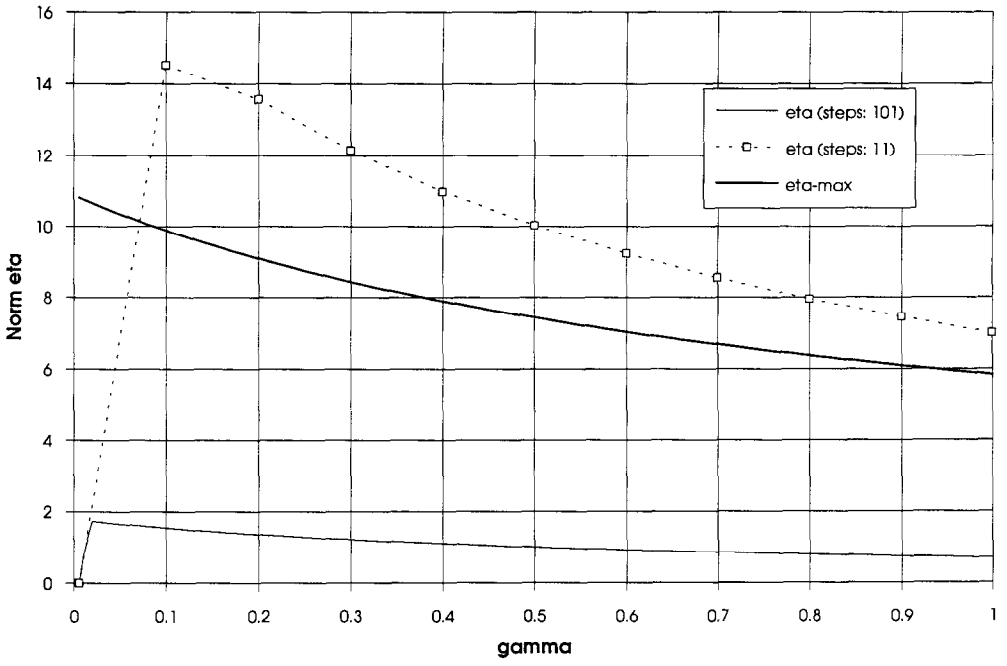

Fig. 9. Simple transverse displacements with isotropic hardening, norm η for $\alpha = 1/2$ and 1 (ratio between plastic strain increment and total elastic strain).

natural strain is approximately $\epsilon \simeq 2$. This maximum strain corresponds to $\dot{\gamma} \simeq 7.0$. We note that for most steels the maximum strain is approximately $\epsilon \simeq 0.7(\dot{\gamma} \simeq 1.5)$. For the pure iron we used the following material parameters

Young's modulus E	210000.0 MPa
Poisson's ratio v	0.27
Yield stress σ_0	130.0 MPa
Hardening modulus H	700.0 MPa. (74)

The shear and normal stresses are given in Figs 13 and 14. In these figures we use the components of the tensor

$$\ln[{}^{t+\Delta t}_{0}\mathbf{U}] = \ln[{}^{t+\Delta t}_{0}\mathbf{R}^{T}\,{}^{t+\Delta t}_{0}\mathbf{X}] \tag{75}$$

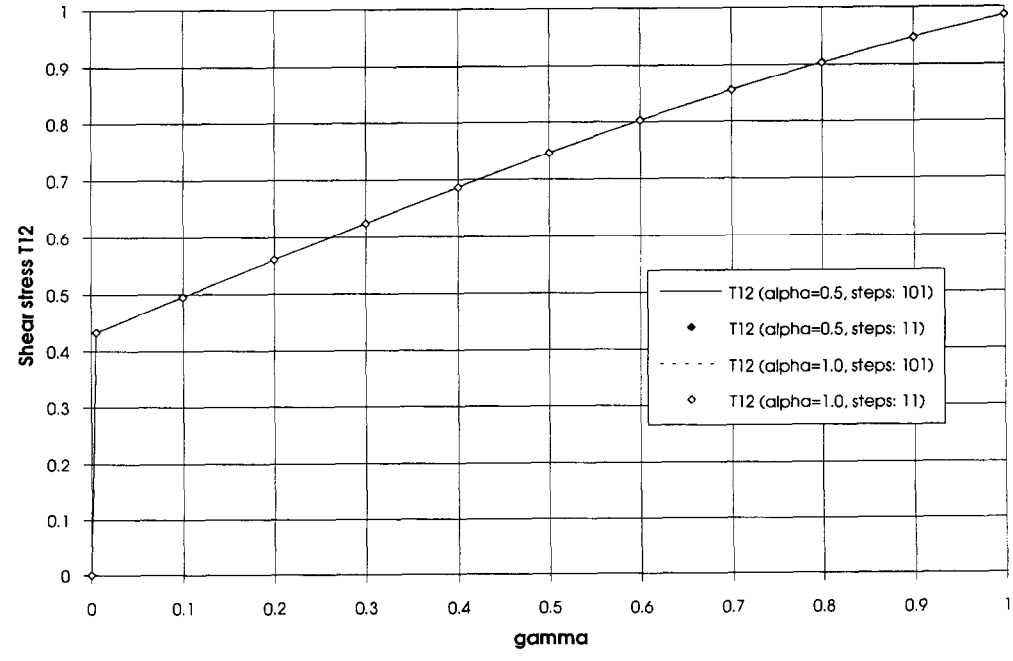

Fig. 10. Simple transverse displacements with kinematic hardening, shear stresses T12 (all stresses are nearly the same).

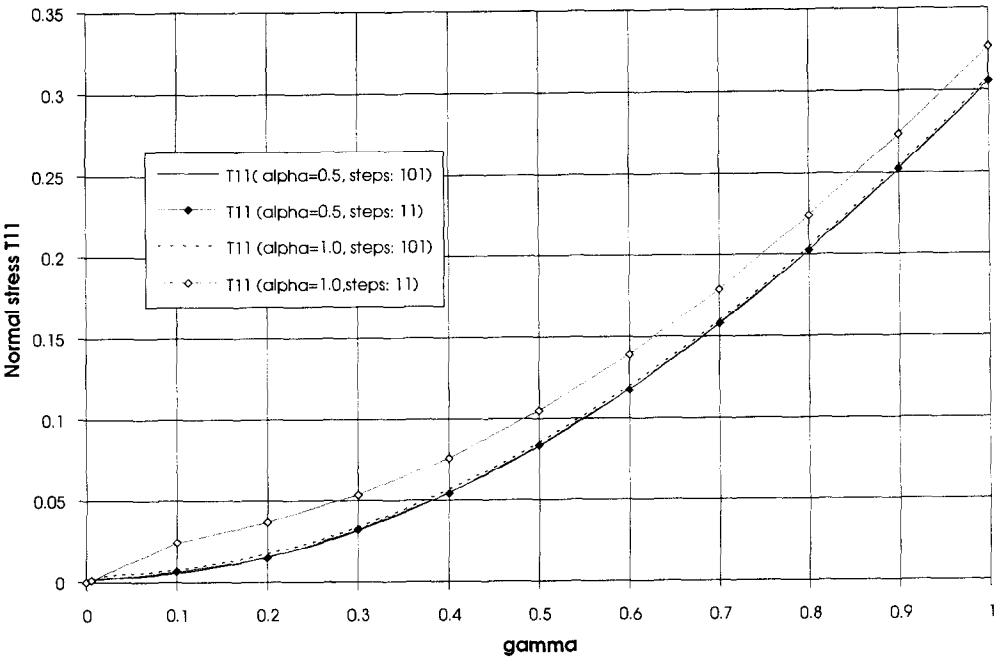

Fig. 11. Simple transverse displacements with kinematic hardening, normal stresses T11.

and call them *component-*(i, j) of the total logarithmic strain tensor.

The norm η is shown in Fig. 15.

4.3. *Simple transverse displacements with additional large rigid rotations (no hardening)*

The following example was given by Weber *et al.* [13]. The material properties are

Young's modulus E	25000.0 MPa
Poisson's ratio ν	0.3
Yield stress σ_0	50.0 MPa. (76)

The stresses in the figures given here are normalized by the *deformation resistance in shear*. The transverse-displacement-rigid rotation deformation is imposed by the deformation gradient

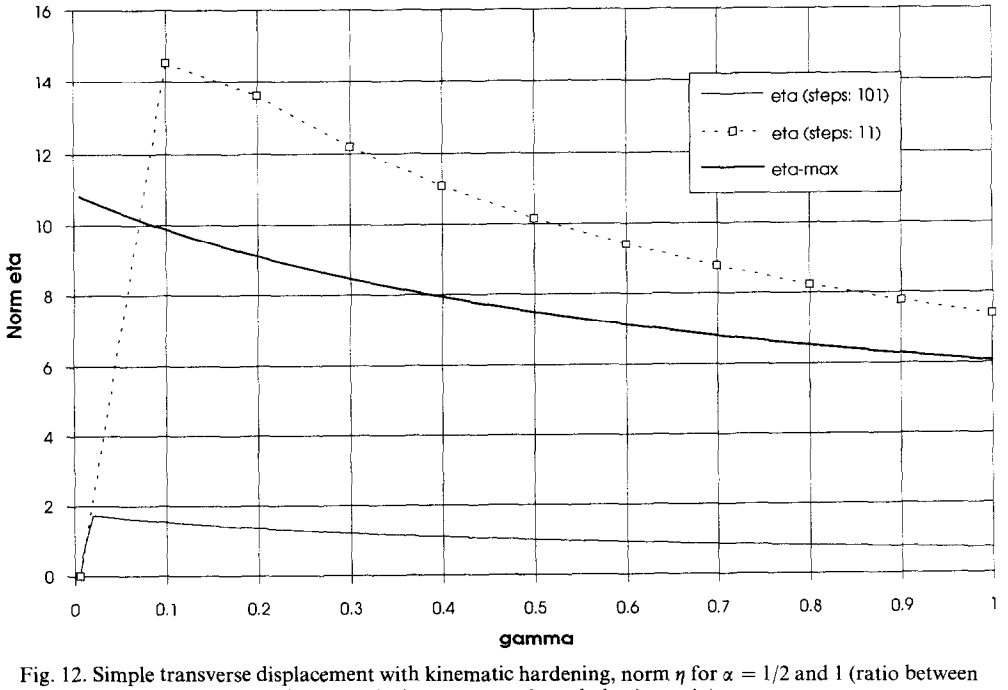

Fig. 12. Simple transverse displacement with kinematic hardening, norm η for $\alpha = 1/2$ and 1 (ratio between plastic strain increment and total elastic strain).

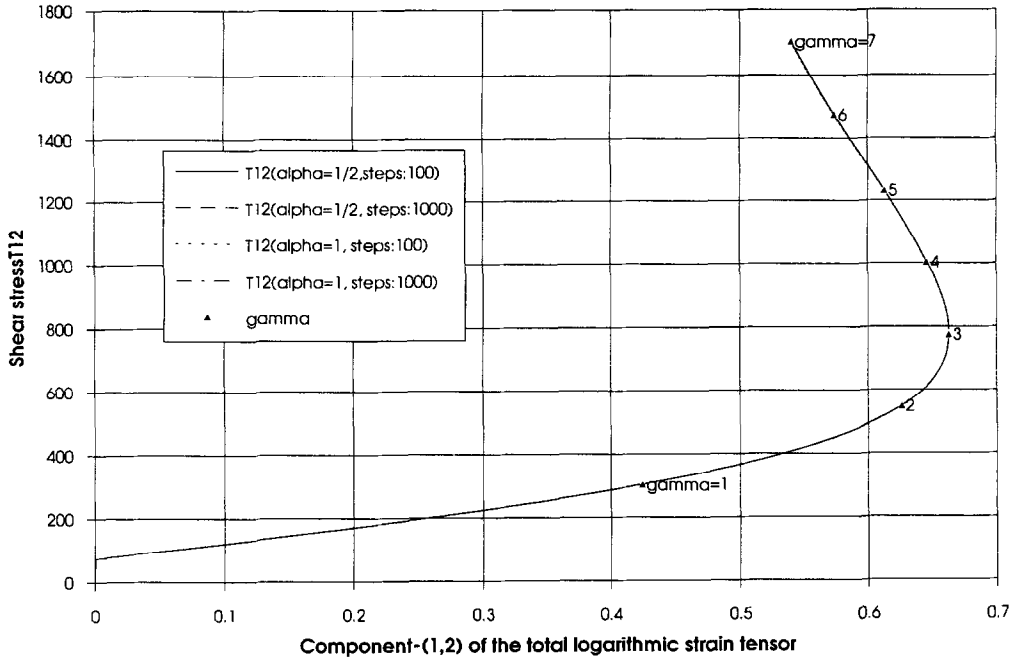

Fig. 13. Pure iron specimen, simple transverse displacements with isotropic hardening, shear stresses (all stresses are nearly the same).

$$\mathbf{X}_{\text{rigid}} = \mathbf{R}_{\text{rigid}}\mathbf{X} = \begin{bmatrix} \cos\omega t & -\sin\omega t & 0 \\ \sin\omega t & \cos\omega t & 0 \\ 0 & 0 & 1 \end{bmatrix} \begin{bmatrix} 1 & \dot{\gamma}t & 0 \\ 0 & 1 & 0 \\ 0 & 0 & 1 \end{bmatrix} \tag{77}$$

with $\omega = 2\pi$ according to a superimposed rigid rotation of 360°. The calculations are compared with solutions obtained using the Hughes–Winget algorithm and an algorithm proposed by Weber *et al.*, see Ref. [13] for these solutions. To make the differences clearer, the calculated stresses are transformed into the rotated 'element'-coordinate system, see Fig. 16. The present algorithm and the algorithm proposed in Ref. [13] are not influenced by the rigid rotation. In large rotation analysis the solution

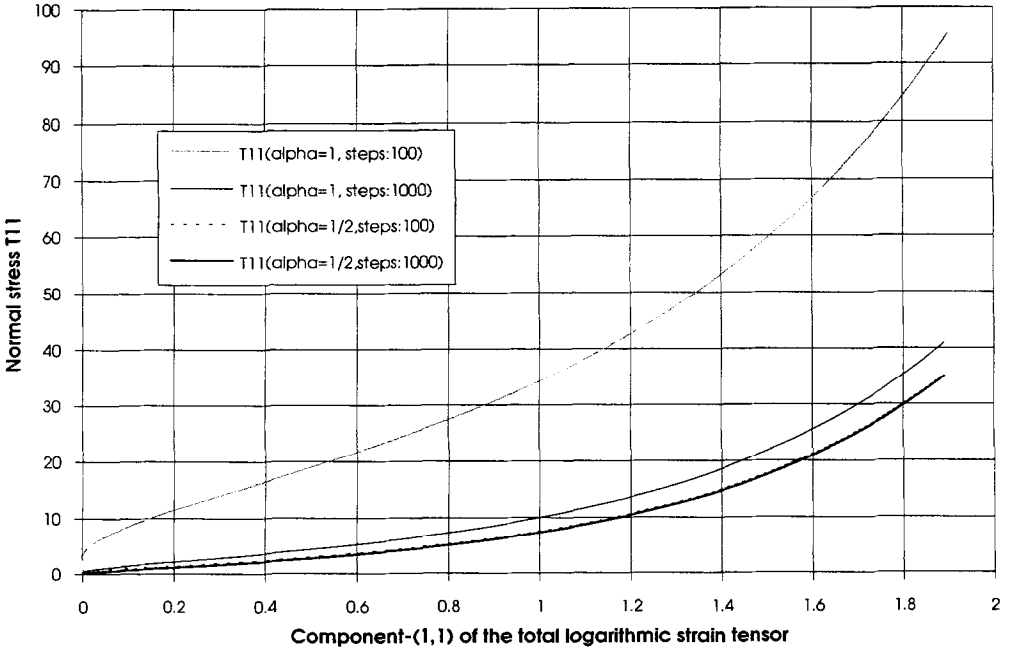

Fig. 14. Pure iron specimen, simple transverse displacement with isotropic hardening, normal stresses.

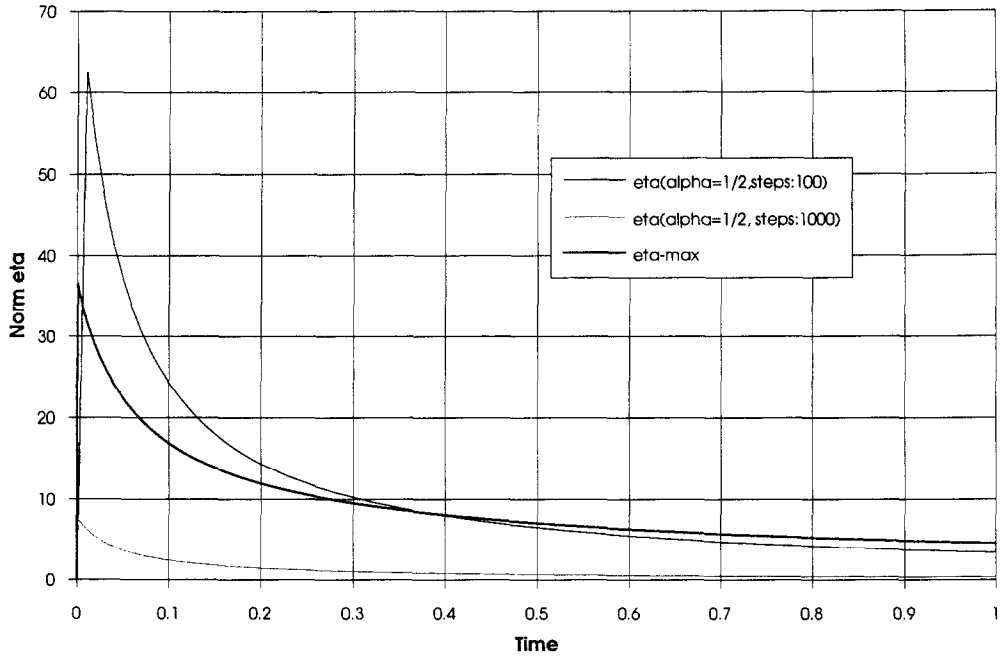

Fig. 15. Pure iron specimen, simple transverse displacements with isotropic hardening, norm η (ratio between plastic strain increment and total elastic strain).

obtainced using the Hughes–Winget algorithm introduces large errors unless small time steps are used.

4.4. *Mixed motion with change of the principal axes of the stress tensor*

This example demonstrates the improvements in our algorithm when $\alpha = \frac{1}{2}$ is used. The deformations considered now are characterized by a significant change of the principal axes of the stretch tensor and stress tensor, respectively. We use the material parameters in eqn (68).

As the rotation tensor plays no critical role in our numerical solution we describe the motion by using

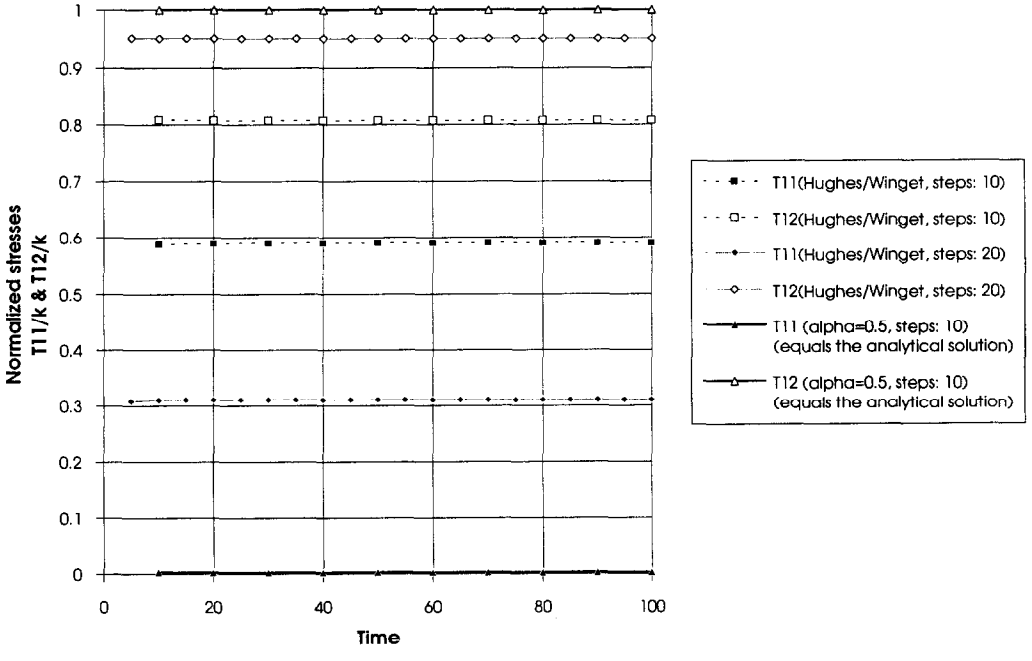

Fig. 16. Simple transverse displacement with superimposed large rigid rotations, Normalized stresses with respect to the element coordinate system.

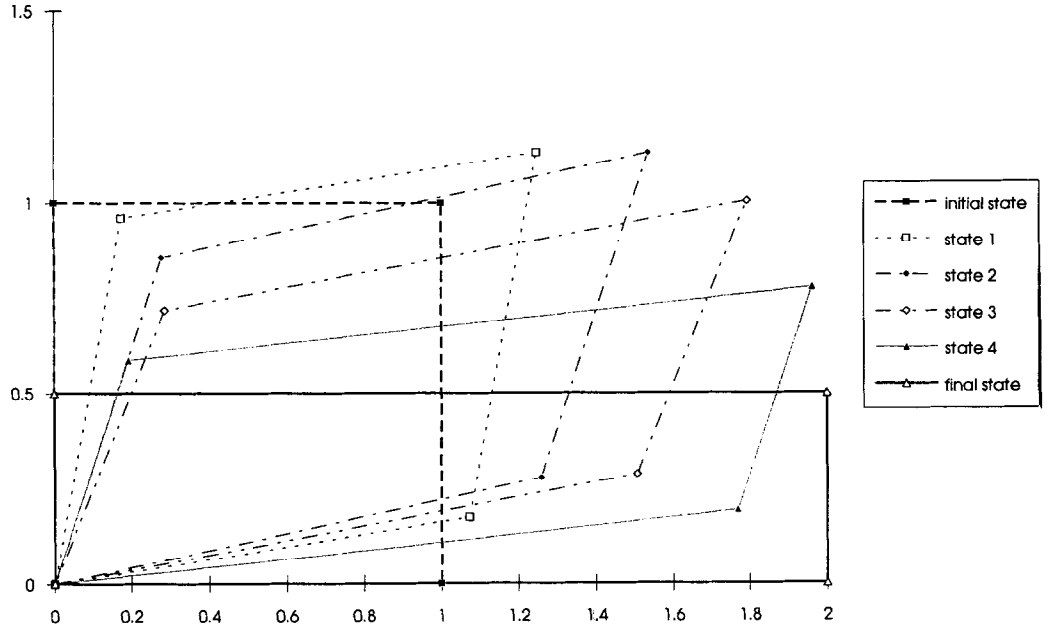

Fig. 17. Mixed motion, deformation pattern.

the symmetric stretch tensor only. This tensor is given by its spectral decomposition

$$\mathbf{U}(t) = \begin{bmatrix} c(t) & -s(t) & 0 \\ s(t) & c(t) & 0 \\ 0 & 0 & 1 \end{bmatrix} \times \begin{bmatrix} \lambda(t) & 0 & 0 \\ 0 & 1/\lambda(t) & 0 \\ 0 & 0 & 1 \end{bmatrix} \times \begin{bmatrix} c(t) & -s(t) & 0 \\ s(t) & c(t) & 0 \\ 0 & 0 & 1 \end{bmatrix}^{\mathrm{T}} \tag{78}$$

with

$$c(t) = \cos \varphi(t)$$

$$s(t) = \sin \varphi(t). \tag{79}$$

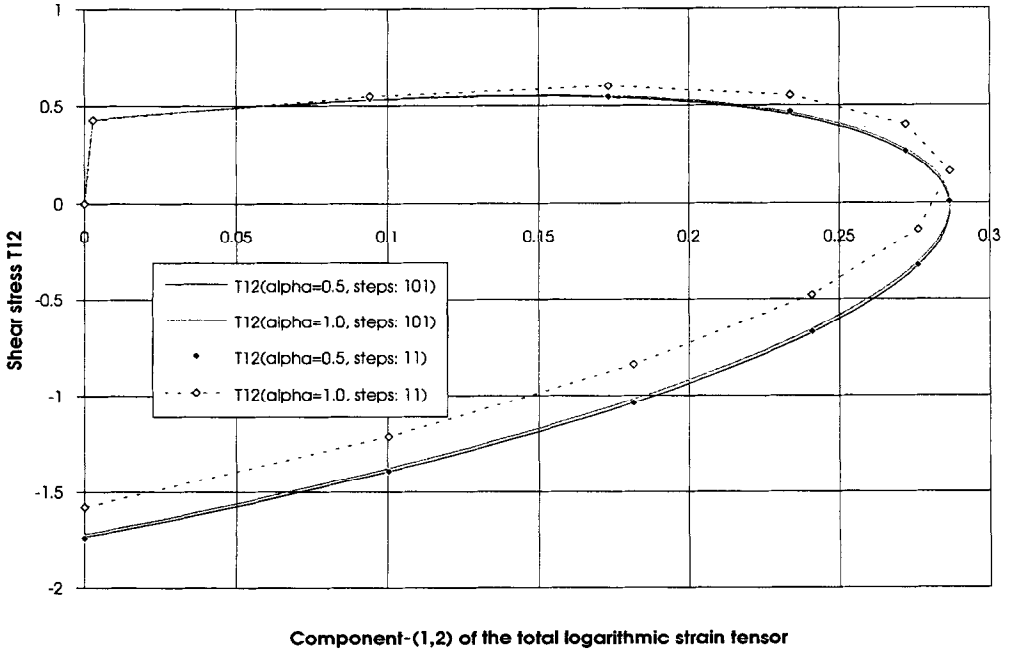

Fig. 18. Mixed motion with increasing stretch, a change of principal axes and isotropic hardening, shear stresses.

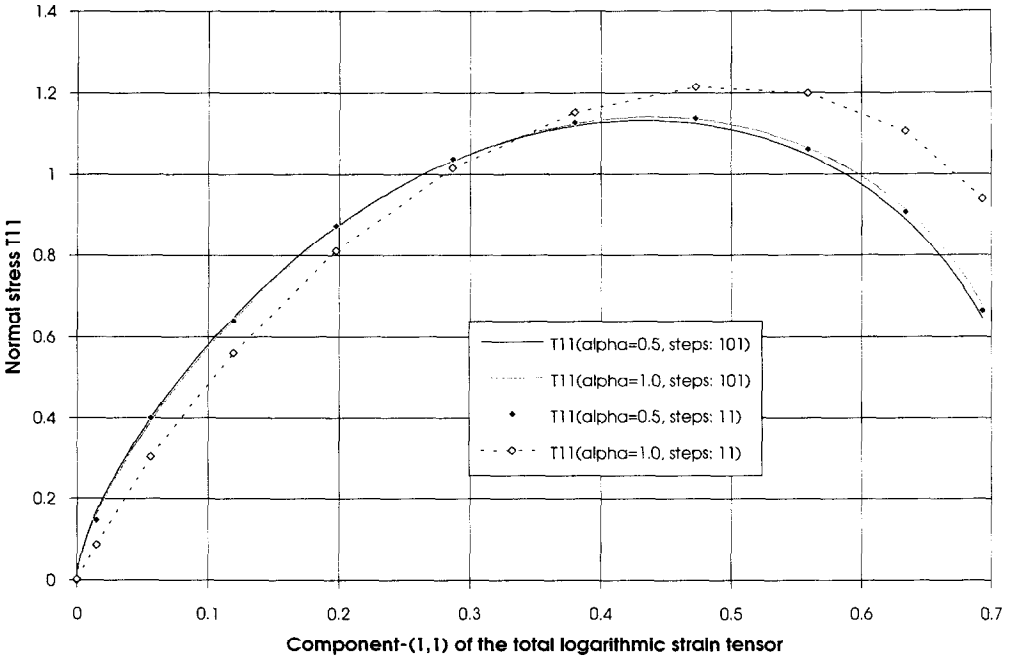

Fig. 19. Mixed motion with increasing stretch, a change of principal axes and isotropic hardening, normal stresses.

We want to describe an isochoric motion which starts with a pure shear and changes over to a simple tension and use $\lambda(t)$ from 1.0 to 2.0 and $\varphi(t)$ from 45° to 0°. Both functions $\lambda(t)$ and $\varphi(t)$ are linear. The pattern of such a deformation is given for certain times in Fig. 17. Considering the initial and final state only, the motion appears to be a simple longitudinal motion. Hence, if only the initial and final states are considered we would expect normal stresses but no shear stresses.

The motion given in this example forces the element to deform in a certain given path. The results presented in Figs 18–20 show that we have normal as well as shear stresses of significant values and of the same order.

We see that the Euler backward procedure using

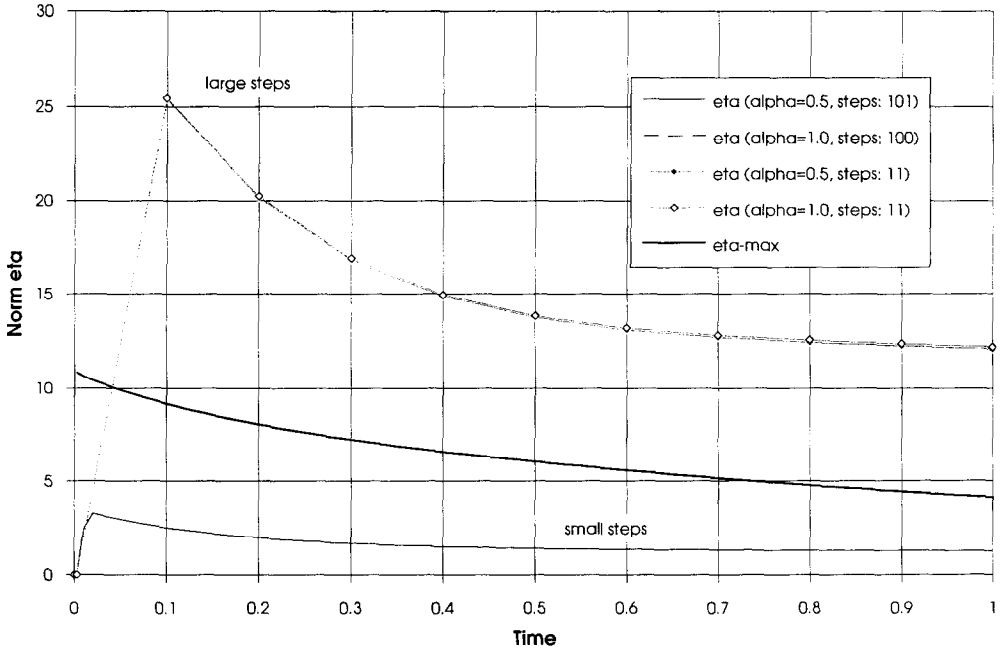

Fig. 20. Mixed motion with increasing stretch, a change of principal axes and isotropic hardening, norm η.

$\alpha = 1$ is able to reproduce the converged solution provided small load steps are used. However, our algorithm using $\alpha = \frac{1}{2}$ is noticeably more accurate and larger time steps can be used.

5. CONCLUSIONS

The results obtained for the elastic–plastic response examples underline the good performance of the algorithm proposed earlier by Eterovic and Bathe [1]. The algorithm works very well for different patterns of elastic–plastic deformations like large normal and shear strains. In particular, large rotations are calculated with good accuracy.

However, if the principal axes of the stretch tensor are changing during the time step, the algorithm produces errors† caused by the inability to follow these changes during the time step. We should note that the solution converges as the time step size is reduced.

The reason for this behavior lies in the approximations contained in the solution of the evolution equation for the plastic deformation gradient, eqn (33). Using the Euler backward procedure ($\alpha = 1$) the plastic strain velocity tensor $\bar{\mathbf{D}}^{\mathrm{p}}$ is assumed to be constant during the time increment. This leads to the often used assumption that the trial and final stress states have the same eigendirections.

Our approach is to solve the governing differential equation in a general form and then use the Euler backward ($\alpha = 1$) or the trapezoidal integration scheme ($\alpha = \frac{1}{2}$).

We have illustrated herein that the solution using $\alpha = \frac{1}{2}$ has better accuracy characteristics. However, even using $\alpha = \frac{1}{2}$ the solution procedure should be restricted to employ a maximum step size. The maximum recommended stepsize is given by an accuracy criterion. Our observations are that we can expect accurate results as long as the plastic strain increments are of the same order as the total elastic strains.

The results presented in this work underline the good performance of the total-deformation based solution procedure for large deformation elastic–plastic analysis.

Acknowledgement—This research was financially supported by a scholarship for Dr G. Gabriel of the German Academic Exchange, Bonn, Germany.

REFERENCES

1. A. L. Eterovic and K. J. Bathe, A hyperelastic-based large strain elasto–plastic constitutive formulation with combined isotropic–kinematic hardening using the logarithmic stress and strain measures. *Int. J. numer. Meth. Engng* **30,** 1099–1114 (1990).
2. K. J. Bathe, *Finite Element Procedures*. Prentice Hall, Englewood Cliffs, NJ (1995).
3. L. Prandtl, Spannungsverteilung in plastischen Körpern. *Proc First Int. Congr. Applied Mechanics* (Edited by C. B. Biezeno and J. M. Burgers), pp. 43–54, Delft (1924).
4. A. Reuss, Berücksichtigung der elastischen Formänderung in der Plastizitätstheorie. *ZAMM* **10,** 266–274 (1930).
5. A. E. Green and P. M. Naghdi, A general theory of an elastic–plastic continuum. *Arch. Rat. mech. Anal.* **18,** 251–281 (1965).
6. K. J. Bathe, M. Kojić and J. Walczak, Some developments in methods for large strain elasto–plastic analysis. *Computational plasticity: Models, Software and Applications I* (Edited by D. J. R. Owen *et al.*), pp. 263–279. Pineridge Press, Swansea (1987).
7. A. L. Eterovic and K. J. Bathe, A note on the use of the additive decomposition of the strain tensor in finite deformation inelasticity. *Comput. Meth. appl. mech. Engng* **93,** 31–38 (1991).
8. E. H. Lee, Elastic–plastic deformation at finite strains. *J. appl. Mech.* **36,** 1–6 (1969).
9. T. J. R. Hughes and J. Winget, Finite rotation effects in numerical integration of rate constitutive equations arising in large deformation analysis. *Int. J. numer. Meth. Engng* **15,** 1862–1867 (1980).
10. M. M. Rashid, Incremental kinematics for finite element applications. *Int. J. numer. Meth. Engng* **36,** 3937–3956 (1993).
11. P. M. Pinsky, M. Ortiz and K. S. Pister, Numerical integration of rate constitutive equations in finite deformation analysis. *Comput. Meth. appl. mech. Engng* **40,** 137–158 (1983).
12. D. P. Flanagan and L. M. Taylor. An accurate numerical algorithm for stress integration with finite rotations. *Comput. Meth. appl. mech. Engng* **62,** 305–320 (1987).
13. G. G. Weber, A. M. Lush, A. Zavaliangos and L. Anand. An objective time-integration procedure for isotropic rate-independent and rate dependent elastic–plastic constitutive equations. *Int. J. Plast.* **6,** 701–744 (1990).
14. S. Nemat-Nasser and Y.-F. Li, A new explicit algorithm for finite-deformation elastoplasticity and elastoviscoplasticity: performance evaluation. *Comput. Struct.* **44,** 937–963 (1992).
15. Y.-F. Li and S. Nemat-Nasser, An explicit integration scheme for finite-deformation plasticity in finite-element methods. *Finite Elements Anal. Des.* **15,** 93–102 (1993).
16. L. H. Wang and S. N. Atluri, An analysis of an explicit algorithm and the radial return algorithm, and a proposed modification, in finite plasticity. *Comput. Mech.* **13,** 380–389 (1994).
17. M. Kojić and K. J. Bathe, Studies of finite element procedures—stress solution of a closed elastic strain path with stretching and shearing using the updated Lagrangian Jaumann formulation. *Comput. Struct.* **26,** 175–179 (1987).
18. K. J. Bathe, E. Ramm and E. L. Wilson, Finite element formulations for large deformation dynamic analysis. *Int. J. numer. Meth. Engng* **9,** 353–386 (1975).
19. J. C. Simo, M. Ortiz, A unified approach to finite deformation elasto–plastic analysis based on the use of hyperelastic constitutive equations. *Comput. Meth. appl. mech. Engng* **49,** 221–245 (1984).
20. J. C. Simo, A framework for finite strain elastoplasticity on maximum plastic dissipation and the multiplicative decomposition. Part I: continuum formulation. *Comput. Meth. appl. mech. Engng* **66,** 199–219 (1988).
21. J. C. Simo, A framework for finite strain elastoplasticity on maximum plastic dissipation and the multiplicative decomposition. Part II: computational aspects. *Comput. Meth. appl. mech. Engng* **68,** 1–31 (1988).

† For the simple transverse displacement motion these errors are at least two orders of magnitude smaller than the shear stresses.

22. J. C. Simo, Algorithms for static and dynamic multiplicative plasticity. *Comput. Meth. appl. Mech. Engng* **99,** 61–112 (1992).
23. B. Moran, M. Ortiz and C. F. Shih, Formulation of implicit finite element methods for multiplicative finite deformation plasticity. *Int. J. numer. Meth. Engng* **29,** 483 514 (1990).
24. G. Weber and L. Anand. Finite deformation constitutive equations and a time integration procedure for isotropic hyperelastic–viscoplastic solids. *Comput. Meth. appl. mech. engng* **79,** 173–202 (1990).
25. D. Peric. On consistent stress rates in solid mechanics: computational implications. *Int. J. numer. Meth. Engng* **33,** 799–817 (1992).
26. D. Peric, A model for finite strain elasto-plasticity based on logarithmic strains: computational issues. *Comput. Meth. appl. mech. Engng* **94,** 35–61 (1992).
27. E. N. Dvorkin, D. Pantuso and E. A. Repetto, A finite element formulation for finite strain elasto–plastic analysis based on mixed interpolation of tensorial components. *Comput. Meth. appl. mech. Engng* **114,** 35–54 (1994).
28. L. Anand, Constitutive equations for hot-working of metals. *Int. J. Plast.* **1,** 213–231 (1985).
29. S. N. Atluri, Alternative stress and conjugate strain measures and mixed variational formulations involving rigid rotations, for computational analyses of finitely deformed solids, with application to plates and shells —I. *Comput. Struct.* **18,** 93–116 (1984).
30. A. Hoger, The stress conjugate to logarithmic strain. *Int. J. Solids Struct.* **23,** 1645–1656 (1987).
31. Y. Dafalias, The plastic spin concept and a simple illustration of its role in finite plastic transformations. *Mech. Mater.* **3,** 223–233 (1984).
32. Y. Dafalias, The plastic spin. *J. appl. Mech.* **52,** 865–875 (1985).
33. A. L. Eterovic and K. J. Bathe, On large strain elasto–plastic analysis with frictional contact conditions. *Rend. Sem. Mat. Univers. Politecn.* Torino, Fasciocolo Speciale (1991).
34. W. C. Moss, Instabilities in large deformation simple shear. *Comput. Meth. appl. mech. Engng* **46,** 329–338 (1984).
35. *ASM Metals Reference Book*. American Society for Metals (1981).
36. W. P. Rees, B. E. Hopkins and H. R. Tipler, Tensile and impact properties of iron and some iron alloys of high purity. *J. Iron Steel Inst.* **169,** 157–168 (1951).

APPENDIX

A. Approximations in the strain relationship

First we analyze the approximation used in eqn (47). We show that the equation represents a good approximation as long as the plastic strain increment is of the same magnitude as the total elastic strain.

From eqn (35) we obtain

$$(\mathbf{X}_*^{\mathrm{E}})^{\mathrm{T}}\mathbf{X}_*^{\mathrm{E}} = \exp\left(\int_t^{t+\Delta t} \bar{\mathbf{D}}^{\mathrm{P}}(\tau)\,\mathrm{d}\tau\right)({}^{t+\Delta t}_{0}\mathbf{X}^{\mathrm{E}})^{\mathrm{T}} \; {}^{t+\Delta t}_{0}\mathbf{X}^{\mathrm{E}} \exp\left(\int_t^{t+\Delta t} \bar{\mathbf{D}}^{\mathrm{P}}(\tau)\,\mathrm{d}\tau\right). \quad \text{(A1)}$$

Considering that

$$(\mathbf{X}_*^{\mathrm{E}})^{\mathrm{T}}\mathbf{X}_*^{\mathrm{E}} = (\mathbf{U}_*^{\mathrm{E}})^{\mathrm{T}}\mathbf{U}_*^{\mathrm{E}} = \exp(2\mathbf{E}_*)$$

$$({}^{t+\Delta t}_{0}\mathbf{X}^{\mathrm{E}})^{\mathrm{T}}\,{}^{t+\Delta t}_{0}\mathbf{X}^{\mathrm{E}} = ({}^{t+\Delta t}_{0}\mathbf{U}^{\mathrm{E}})^{\mathrm{T}}\,{}^{t+\Delta t}_{0}\mathbf{U}^{\mathrm{E}} = \exp(2\,{}^{t+\Delta t}\mathbf{E}^{\mathrm{E}}) \quad \text{(A2)}$$

equation (A1) becomes

$$\exp(2\mathbf{E}_*) = \exp\left(\int_t^{t+\Delta t} \bar{\mathbf{D}}^{\mathrm{P}}(\tau)\,\mathrm{d}\tau\right)\exp(2\,{}^{t+\Delta t}\mathbf{E}^{\mathrm{E}}) \times \exp\left(\int_t^{t+\Delta t} \bar{\mathbf{D}}^{\mathrm{P}}(\tau)\,\mathrm{d}\tau\right). \quad \text{(A3)}$$

For simplicity of presentation let us use the notation

$$\exp(2\mathbf{E}_*) = \exp(\epsilon\,\mathbf{D})\exp(2\mathbf{E})\exp(\epsilon\,\mathbf{D}) \quad \text{(A4)}$$

instead of eqn (A3), where ϵ stands for a typical stepsize and $\epsilon\,\mathbf{D}$ for the integral. For now, we assume that the integral is evaluated accurately, and we solely focus our attention on the difference between eqns (47) and (A4).

The tensor logarithm and the tensor exponential of any second order tensor may be replaced by the series

$$\exp(\mathbf{X}) = \sum_{n=0}^{\infty} \frac{\mathbf{X}^n}{n!} \quad \text{for any } \mathbf{X} \quad \text{(A5)}$$

$$\ln(\mathbf{1}+\mathbf{Y}) = \sum_{n=0}^{\infty} \frac{(-1)^n}{(n+1)}\mathbf{Y}^{n+1} \quad \text{for } \|\mathbf{Y}\| \ll \mathbf{1}. \quad \text{(A6)}$$

Let us define a tensor $\mathbf{E}_0$

$$\mathbf{E}_0 = \tfrac{1}{2}(\exp(2\mathbf{E}) - \mathbf{1}) \quad \text{(A7)}$$

and describe higher order terms by the following norms

$$(\epsilon\,\mathbf{D})^i \to \mathrm{O}(\|\epsilon\,\mathbf{D}\|)^i$$

$$\mathbf{E}^i \simeq \mathbf{E}_0^i \to \mathrm{O}(\|\mathbf{E}\|)^i. \quad \text{(A8)}$$

The ratio of both norms is given by

$$\eta = \frac{\mathrm{O}\|\epsilon\,\mathbf{D}\|}{\mathrm{O}\|\mathbf{E}\|}. \quad \text{(A9)}$$

It follows from eqn (A5) that

$$\exp(\epsilon\,\mathbf{D}) = \mathbf{1} + \epsilon\,\mathbf{D} + \tfrac{1}{2}(\epsilon\,\mathbf{D})^2 + \mathrm{O}(\|\epsilon\,\mathbf{D}\|)^3. \quad \text{(A10)}$$

Then, using eqn (A7), eqn (A4) can be rewritten as

$$\exp(2\mathbf{E}_*) = \mathbf{1} + 2\mathbf{E}_0 + 2\epsilon\,\mathbf{D} + 2\mathbf{E}_0\epsilon\,\mathbf{D} + 2\epsilon\,\mathbf{D}\mathbf{E}_0 + 2(\epsilon\,\mathbf{D})^2 + \mathrm{O}(\|\mathbf{E}_0\|)\mathrm{O}(\|\epsilon\,\mathbf{D}\|)^2 + \mathrm{O}(\|\epsilon\,\mathbf{D}\|)^3 \quad \text{(A11)}$$

For sufficiently small $\|\mathbf{E}_0\|$ and $\|\epsilon\,\mathbf{D}\|$ this equation allows the series expansion

$$2\mathbf{E}_* = \sum_{n=0}^{\infty} \frac{(-1)^n}{(n+1)}[2\mathbf{E}_0 + 2\epsilon\,\mathbf{D} + 2\mathbf{E}_0\epsilon\,\mathbf{D} + 2\epsilon\,\mathbf{D}\mathbf{E}_0 + 2(\epsilon\,\mathbf{D})^2]^{n+1} + \mathrm{O}(\|\mathbf{E}_0\|)\mathrm{O}(\|\epsilon\,\mathbf{D}\|)^2 + \mathrm{O}(\|\epsilon\,\mathbf{D}\|)^3 \quad \text{(A12)}$$

and it turns out that

$$\mathbf{E}_* = \mathbf{E} + \epsilon\,\mathbf{D} + \eta\,\mathrm{O}(\|\mathbf{E}\|)^3 + \eta^2\mathrm{O}(\|\mathbf{E}\|)^3 + \eta^3\mathrm{O}(\|\mathbf{E}\|)^3. \quad \text{(A13)}$$

It is easy to see that equation (A13) allows a second-order-accurate approximation using

$$\mathbf{E}_* = \mathbf{E} + \epsilon\,\mathbf{D}. \quad \text{(A14)}$$

The validity of this approximation depends obviously on the value of η. Assuming that $\eta \geqslant 1$ the critical value is given by the term containing η^3. We are able to determine the maximum allowable η comparing this term with the order

of the total elastic strain. If we want this term to be at least two orders smaller than the elastic strains we should use

$$\eta \leqslant \eta_{\text{max. allowable}} = \sqrt[3]{\frac{1}{10^2 \cdot O(\|\mathbf{E}\|)^2}}. \tag{A15}$$

It is obvious that the maximum allowable η depends on the order of the elastic strains. The larger the elastic strains, the smaller the value of η should be.

The other restriction is given by the approximation used to obtain $\epsilon\mathbf{D}$ (see eqns (51)–(54)). We have not been able as yet to estimate the error introduced in this approximation.

However, our numerical examples show that we can expect good results with a maximum relative error of less than approximately 0.1% using $\eta \cong 1$ and $\alpha = \frac{1}{2}$. The error will increase to approximately 1% using $\alpha = 1$. We note that in some situations we can obtain accurate results using much larger values of η.

However, for practical calculations we suggest to work in the region

$$\eta = \frac{O\|\epsilon\mathbf{D}\|}{O\|\mathbf{E}\|} \simeq 1 \tag{A16}$$

where we can usually expect sufficiently accurate results. This equation means that the plastic strain increment should be of the same order as the total elastic strain.

We now show that the trial elastic rotation tensor is approximately equal to the final elastic rotation tensor for any value of α.

Using eqn (46) we define

$${}^{t+\Delta t}_{0}\mathbf{R}^{\mathrm{E}} = \mathbf{R}^{\mathrm{E}}_{*}\mathbf{R}_{c} \tag{A17}$$

with the rotational correction

$$\mathbf{R}_{c} = \exp(\mathbf{E}^{\mathrm{E}}_{*})\exp\left(-\int_{t}^{t+\Delta t}\bar{\mathbf{D}}^{\mathrm{P}}(\tau)\,\mathrm{d}\tau\right)\exp(-{}^{t+\Delta t}_{0}\mathbf{E}^{\mathrm{E}}) \tag{A18}$$

For convenience we write this equation as

$$\mathbf{R}_{c} = \exp(\mathbf{E}_{*})\exp(-\epsilon\mathbf{D})\exp(-\mathbf{E}). \tag{A19}$$

Using eqn (84) it follows that

$$\begin{aligned}\mathbf{R}_{c} = \mathbf{I} &+ (\mathbf{E}_{*} - \mathbf{E} - \epsilon\mathbf{D}) + \tfrac{1}{2}(\mathbf{E}_{*} - \mathbf{E} - \epsilon\mathbf{D})^{2} \\ &+ \tfrac{1}{2}([\epsilon\mathbf{D}, \mathbf{E}] + [\mathbf{E}, \mathbf{E}_{*}] + [\epsilon\mathbf{D}, \mathbf{E}_{*}]) \\ &+ O(\|\mathbf{E}_{*}\|)^{3}.\end{aligned} \tag{A20}$$

Because of the relation (93) it is easy to see that

$$\begin{aligned}\mathbf{R}_{c} = \mathbf{I} + \tfrac{1}{2}((\epsilon\mathbf{D}\mathbf{E} - \mathbf{E}\,\epsilon\mathbf{D}) + (\mathbf{E}\mathbf{E}_{*} - \mathbf{E}_{*}\mathbf{E}) \\ + (\epsilon\mathbf{D}\mathbf{E}_{*} - \mathbf{E}_{*}\,\epsilon\mathbf{D})).\end{aligned} \tag{A21}$$

It follows from this equation that as long as all terms commute, the rotational correction $\mathbf{R}_{c}$ is equal to the identity. If this is not the case, deviations from the identity matrix occur that are small compared to $\mathbf{I}$ as long as we work in the suggested time step region. Inaccuracy may only occur using very large time steps.